Angular Band Structure of a Vortex Line in a Type-II Superconductor

François Gygi and Michael Schluter
AT&T Bell Laboratories, 600 Mountain Avenue, Murray Hill, New Jersey 07974
(Received 6 July 1990)

The electronic structure of a vortex line in a type-II superconductor is calculated in the low-magnetic-field limit in the framework of the Bogoliubov–de Gennes theory. It is found that breaking the rotational invariance of a vortex line by means of either an anisotropic crystal potential or the presence of neighboring vortices induces an *angular* band structure in the low-energy part of the quasiparticle spectrum. The associated quasiparticle amplitudes become distorted and exhibit a characteristic "star" shape whose orientation is energy dependent. This explains recent scanning-tunneling-microscopy experiments by Hess, Robinson, and Waszczak [Phys. Rev. Lett. **64**, 2711 (1990)] on $NbSe_2$.

PACS numbers: 74.50.+r, 61.16.Di, 74.60.−w

Recent scanning-tunneling-microscopy (STM) experiments on $NbSe_2$ by Hess and co-workers[1] have given a new insight into the detailed structure of vortex lines in type-II superconductors. Besides showing the enhancement in the zero-bias tunneling conductance caused by the presence of bound states in the vortex core, these experiments have also provided images of vortex lines in which the contours of equal tunneling conductance have a characteristic star shape. Most strikingly, the orientation of these star-shaped patterns relative to the triangular flux lattice was found to depend on the tunneling bias voltage. At zero bias, the measured tunneling conductance decays rapidly in the direction of the nearest-neighboring vortex lines, and more slowly in a direction 30° away from the nearest neighbors; i.e., the arms of the star pattern point towards the interstitial sites. At a bias voltage of 0.5 mV, which corresponds to approximately half of the zero-field superconducting gap Δ_0, the situation is reversed and the tunneling conductance decays more slowly in the direction of the nearest-neighboring vortex lines; i.e., the stars are rotated by 30° (see Fig. 1, left-hand side). In this paper we show that the observed star-shaped pattern and its rotation can be explained in terms of the solutions of the Bogoliubov–de Gennes equations using a simplified two-band model.

Early descriptions of an isolated vortex line based on the microscopic theory of Gor'kov[2] and Bogoliubov and de Gennes[3] have been given by Caroli, de Gennes, and Matricon[4,5] and Bardeen *et al.*[6] These authors were able to solve the Bogoliubov–de Gennes equations approximately in various limits. More recently, these equations were solved numerically for bound states alone[7] and for bound and scattering states,[8] which allowed explanation of the tunneling spectra observed at the vortex core by Hess and co-workers. Fully self-consistent solutions for the isolated isotropic vortex have been obtained subsequently[9] which provide the detailed structure of the gap function at low temperature as well as the structure of the tunneling conductance spectrum at various distances away from a vortex line.

The electronic structure of a superconductor is described in terms of spinors

$$\psi_n(\mathbf{r}) = \begin{pmatrix} u_n(\mathbf{r}) \\ v_n(\mathbf{r}) \end{pmatrix} \tag{1}$$

which satisfy the Bogoliubov–de Gennes[3] equation

$$\left\{ \sigma_z \left[\frac{1}{2m} [\mathbf{p} - \sigma_z \frac{e}{c} \mathbf{A}(\mathbf{r})]^2 + U(\mathbf{r}) \right] + [\Delta(\mathbf{r})\sigma_+ + \Delta^*(\mathbf{r})\sigma_-] \right\} \psi_n(\mathbf{r}) = E_n \psi_n(\mathbf{r}) , \tag{2}$$

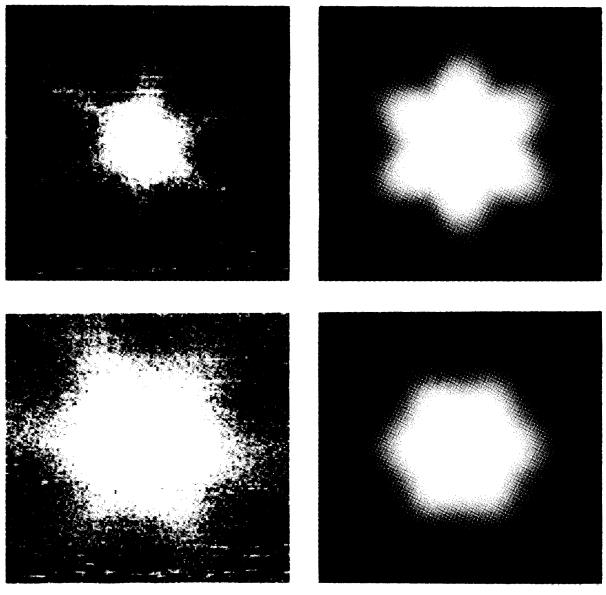

FIG. 1. Tunneling conductance images at zero bias (top row) and at finite bias (bottom row). The left-hand column shows the experimental results of Ref. 1. Calculated images are shown on the right-hand column. The nearest-neighbor direction of the Abrikosov flux lattice is the horizontal direction.

where $\sigma_\pm = \frac{1}{2}(\sigma_x \pm i\sigma_y)$, σ_x, σ_y, and σ_z are Pauli matrices, $U(\mathbf{r})$ is the one-particle crystal potential, $\Delta(\mathbf{r})$ is the gap function, and $\mathbf{A}(\mathbf{r})$ is the vector potential.

In the case of an isolated vortex line, and in the absence of any anisotropic crystal potential, the system is invariant under all rotations above the z axis, and angular momentum can be used as a quantum number. Using cylindrical coordinates and choosing the gauge in which $\Delta(\mathbf{r}) = |\Delta(\mathbf{r})| e^{-i\theta}$, the quasiparticle amplitudes can be written as

$$\psi^{(0)}_{n\mu k_z}(\mathbf{r}) = \begin{pmatrix} u_{n\mu k_z}(r) e^{i(\mu - 1/2)\theta} \\ v_{n\mu k_z}(r) e^{i(\mu + 1/2)\theta} \end{pmatrix} e^{ik_z z}, \tag{3}$$

where the angular momentum μ is *half* an odd integer. We assume a k_z-independent Fermi surface, which is appropriate in the case of $NbSe_2$.

First, we consider perturbations to a cylindrically symmetric vortex caused by the presence of an anisotropic crystal potential described by $H_1 = \delta U(\mathbf{r})\sigma_z$. The isotropic component of the crystal potential can be accommodated by using an effective mass in the isotropic kinetic-energy operator. The additional term we consider here describes the angular-dependent part, i.e., the anisotropy of the effective mass. In the case of $NbSe_2$ this term has hexagonal symmetry. Its precise value is not known, and is affected by the presence of a hexagonal charge-density wave at low temperature.

Second, we consider the presence of neighboring vortices, which can be accounted for by modifying the vector potential in the vicinity of the vortex line

$$\mathbf{A}(\mathbf{r}) = \mathbf{A}^{(0)}(r) + \delta\mathbf{A}(r,\theta). \tag{4}$$

The lowest-order magnetic perturbation to the Bogoliubov-de Gennes Hamiltonian is

$$H_2 = -\frac{e}{2mc}[\delta\mathbf{A}\cdot\mathbf{p} + \mathbf{p}\cdot\delta\mathbf{A}] I_\sigma + \frac{e^2}{mc^2}[\delta\mathbf{A}\cdot\mathbf{A}^{(0)}]\sigma_z, \tag{5}$$

where I_σ is the identity matrix in spin space. The crystal potential $\delta U(\mathbf{r})$ in H_1 and the last term in Eq. (5) both appear in front of a σ_z operator, which implies that they are not pair breaking to first order. On the other hand, the first term in Eq. (5) is pair breaking to first order and should be dominant. However, especially at low magnetic field, the crystal potential may dominate, so that all contributions must be kept in our analysis.

Since we are mainly interested in the changes occurring in the low-energy part of the spectrum—i.e., $E < \Delta_0$—we expand the Hamiltonian in the bound states of the unperturbed problem. The sixfold symmetry of the perturbation simplifies the problem considerably. Only bound states whose angular momentum differ by $\delta\mu = 6$ are coupled by the perturbation. If we consider only the subspace spanned by the twelve lowest bound states, i.e., the bound states $\mu = \frac{1}{2}$ to $\frac{23}{2}$, which is reasonable at low energy, the Hamiltonian reduces to a block-diagonal matrix. Each block is a 2×2 matrix of the form

$$H_\mu = \begin{pmatrix} \langle\mu|H|\mu\rangle & \langle\mu|H|\mu+6\rangle \\ \langle\mu+6|H|\mu\rangle & \langle\mu+6|H|\mu+6\rangle \end{pmatrix} \equiv \begin{pmatrix} E^{(0)}_\mu & W_\mu \\ W_\mu & E^{(0)}_{\mu+6} \end{pmatrix}. \tag{6}$$

Note that due to the absence of rotational symmetry, the quantum number μ is now limited to values $\frac{1}{2} \le \mu \le \frac{11}{2}$ and only serves to label the irreducible representations of the sixfold rotation group C_6. It is not an eigenvalue of the angular momentum operator anymore. The eigenvalues of H_μ form two bands, labeled + and −, which are separated by an energy gap of order $|W_{1/2}| + |W_{11/2}|$ in this subspace spanned by the twelve lowest bound states. This gap might be reduced if higher-energy bound states are included in the basis set. The crossover from the lower to the upper bound occurs at an energy

$$E^{(0)}_{11/2} < E_c < E^{(0)}_{13/2}. \tag{7}$$

The tunneling conductance can be calculated in the simplest approximation[8] using the expression

$$\frac{\partial I(\mathbf{r},V)}{\partial V} \propto \sum_i [|u_i(\mathbf{r})|^2 f'(E_i - eV) + |v_i(\mathbf{r})|^2 f'(E_i + eV)], \tag{8}$$

where $f'(E)$ is the derivative of the Fermi distribution, and i denotes all quantum numbers. Contrary to the isolated vortex case, the conductance has now lost its cylindrical symmetry. For example, in the lower band, we have

$$|u_\mu^-(\mathbf{r})|^2 = \alpha_\mu^2 |u_\mu(r)|^2 + \beta_\mu^2 |u_{\mu+6}(r)|^2 - 2\alpha_\mu\beta_\mu |u_\mu(r)||u_{\mu+6}(r)|\cos 6\theta, \tag{9}$$

where α_μ and β_μ are the components of the eigenvectors of H_μ. The last term in Eq. (9) introduces an angular (sixfold) modulation in the tunneling conductance. The STM image of a vortex line therefore exhibits a star shape. The orientation of this star-shaped conductance pattern changes with the coefficients α_μ and β_μ which in turn depend on the value of the tunneling bias voltage. At small bias, the tunneling process occurs in the lower band whose eigenfunctions have an angular "bonding" character, whereas at a bias larger than E_c, the tunneling process involves the upper band which has "antibonding" character. The sixfold angular modulation of the conductance is therefore reversed as the bias increases from zero to above E_c; i.e., the star pattern rotates by 30°.

The *absolute* orientation of the conductance patterns is determined by the relative magnitude of the perturbations H_1 and H_2 in a given direction. The sign of H_1 is *a priori* unknown but can in principle be obtained from de-

tailed band-structure calculations. In deriving the sign of H_2, we assume that the vector potential of the vortex lattice is the sum of the vector potentials of isolated vortices (which is appropriate in the low-field limit). We then find that the perturbation can be approximated by

$$\delta\mathbf{A}(r,\theta)=\begin{pmatrix}\delta A_r(r)\sin 6\theta\\ \delta A_\theta^{(1)}(r)+A_\theta^{(2)}(r)\cos 6\theta\end{pmatrix}, \qquad (10)$$

where $\theta=0$ is the nearest-neighbor direction of the Abrikosov lattice. The corresponding magnetic field has maxima in the nearest-neighbor directions. Retaining only the magnetic perturbation H_2, and solving the 2×2 secular problem numerically, we find that the resulting zero-bias star has arms extending towards the nearest-neighboring vortices, i.e., in the directions where the magnetic field is stronger. This is consistent with the picture of the lowest bound states extending preferentially into the regions where the magnetic field is strongest, i.e., where the gap is more strongly suppressed. This is, however, *not* the orientation of the star observed experimentally at low field. We therefore conclude that, in the low-field limit, the crystal potential H_1 is dominant, so that the total perturbation H_1+H_2 is repulsive in the nearest-neighbor direction, and attractive in the interstitial direction. In other words, the orientation of the stars in $NbSe_2$ seems to be determined by the underlying crystal potential and not by the Abrikosov flux lattice. The relative magnitude of the matrix elements of H_1 and H_2 depends on μ. At large μ and not too small fields, the increasing magnetic perturbation may cause the matrix element W_μ to change sign. This would result in an additional distortion of the star-shaped pattern at large distances from the core, where the contributions to the conductance from states with large μ become important. Details will be discussed in a forthcoming paper.[9]

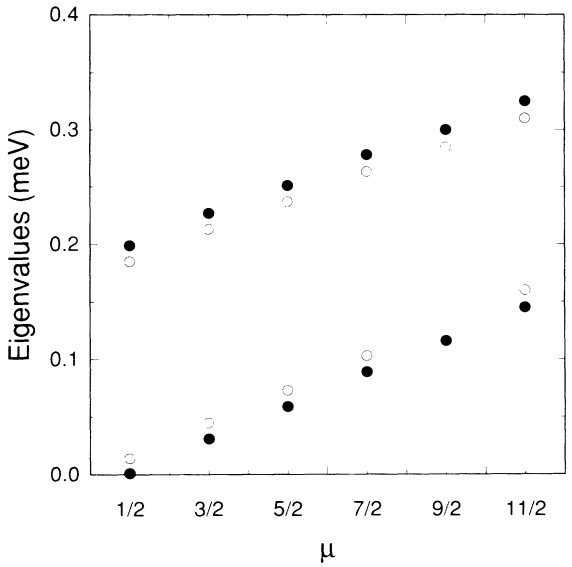

FIG. 2. Low-energy part of the quasiparticle spectrum of a vortex line in the cylindrically symmetric case (open circles) and in the presence of a sixfold-symmetric perturbation (solid circles).

We have calculated the conductance as a function of

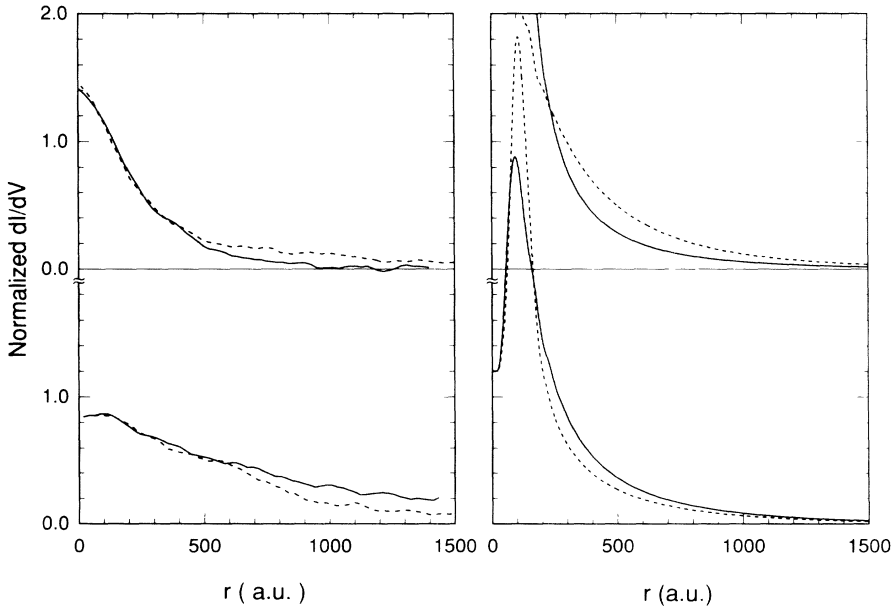

FIG. 3. Tunneling differential conductance calculated at zero bias (top right) and at a finite bias of $V=\Delta_0/5$ (bottom right) in the direction of the nearest-neighboring flux line (solid lines) and in the interstitial direction (dashed lines). The experimental results from Ref. 1 are shown in the left panels.

distance from the vortex core, assuming a value of $|W_\mu|/\Delta_0=0.05$, independent of μ. This value is comparable to the energy spacing between the lowest quasiparticle bound states of the isolated vortex. The resulting modified spectrum is shown in Fig. 2, together with the unperturbed spectrum. The quasiparticle amplitudes used in the calculation of the conductance were obtained from a self-consistent calculation of the electronic structure of an isolated vortex.[9] The conductance profiles calculated in the direction of the nearest-neighboring vortex and in the interstitial direction are shown in Fig. 3 at both zero bias and a bias of $\Delta_0/5$, which corresponds to the bottom of the lower and of the upper bands, respectively (see Fig. 2). The experimental curves of Ref. 1 are also shown in Fig. 3 for comparison. Our simple two-band model correctly predicts the reversal of the anisotropy of the tunneling conductance between low and high bias voltages, as can be seen by comparing the solid and dashed lines. The enhanced zero-bias conductance at the vortex core, also shown in Fig. 3, is exaggerated in the calculated conductance, as already discussed in Refs. 7 and 8. Finally, we used the calculated conductance $\partial I(r,\theta,V)/\partial V$ to produce a gray-scale image, similar to the experimental image of Ref. 1. It is compared to experiment in Fig. 1 (right-hand column), illustrating dramatically the effects of our simple model.

In conclusion, we have shown that in the presence of a hexagonal crystal field and of the neighboring vortices of the Abrikosov lattice, the STM tunneling conductance exhibits a sixfold-symmetric star shape in the vicinity of a flux line. By means of a simple two-band model, we have also shown that the orientation of this star-shaped pattern depends on the tunneling bias voltage, and that it rotates by 30° at a critical value of the bias voltage. Comparison of the absolute star orientation with experiment leads to the conclusion that the underlying crystal potential, and not the Abrikosov flux lattice, is the main source for the observed anisotropy.

We would like to thank H. Hess for many fruitful discussions, and for communicating his results to us prior to publication. One of us (F.G.) acknowledges financial support from the Swiss National Science Foundation.

[1]H. Hess, R. B. Robinson, and J. V. Waszczak, Phys. Rev. Lett. **64**, 2711 (1990); H. Hess, R. B. Robinson, R. C. Dynes, J. M. Valles, Jr., and J. V. Waszczak, Phys. Rev. Lett. **62**, 214 (1989); J. Vac. Sci. Technol. A **8**, 450 (1990).

[2]L. P. Gor'kov, Zh. Eksp. Teor. Fiz. **36**, 1918 (1959) [Sov. Phys. JETP **9**, 1364 (1959)].

[3]See, e.g., P. G. de Gennes, *Superconductivity of Metals and Alloys* (Addison-Wesley, Reading, MA, 1989).

[4]C. Caroli, P. G. de Gennes, and J. Matricon, Phys. Lett. **9**, 307 (1964).

[5]C. Caroli and J. Matricon, Phys. Kondens. Mater. **3**, 380 (1965); C. Caroli, Ann. Inst. Henri Poincaré, Sect. A **4**, 159 (1966).

[6]J. Bardeen, R. Kümmel, A. E. Jacobs, and L. Tewordt, Phys. Rev. **187**, 556 (1969).

[7]J. D. Shore, M. Huang, A. T. Dorsey, and J. P. Sethna, Phys. Rev. Lett. **62**, 3089 (1989).

[8]F. Gygi and M. Schlüter, Phys. Rev. B **41**, 822 (1990).

[9]F. Gygi and M. Schlüter (to be published).

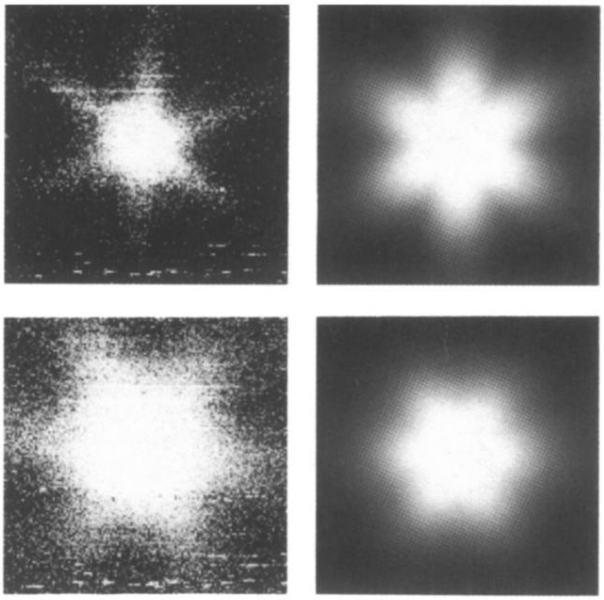

FIG. 1. Tunneling conductance images at zero bias (top row) and at finite bias (bottom row). The left-hand column shows the experimental results of Ref. 1. Calculated images are shown on the right-hand column. The nearest-neighbor direction of the Abrikosov flux lattice is the horizontal direction.